*Int. J. Solids Structures* Vol. 22, No. 12, pp. 1571–1578, 1986
Printed in Great Britain.

0020–7683/86 $3.00 + .00
Pergamon Journals Ltd.

# PERIODIC NECKING INSTABILITIES IN LAYERED PLASTIC COMPOSITES

PAUL S. STEIF
Department of Mechanical Engineering, Carnegie-Mellon University, Pittsburgh, PA 15213, U.S.A.

(*Received* 9 *April* 1985; *in revised form* 7 *November* 1985)

**Abstract**—A bifurcation analysis of a solid composed of alternating material layers is carried out. We study the conditions under which periodic incremental deformations (eigenmodes), consistent with an overall homogeneous stretching, can emerge when the solid is subjected to plane strain, uniaxial tension parallel to the layer interfaces. These undulatory eigenmodes are in competition with shear localization, taken here to be signaled by a loss of ellipticity of the governing incremental equations. The influence of various material parameters on this competition is discussed and contact is made with previous work.

## 1. INTRODUCTION

When subjected to large strains, solids consisting of layers of alternating material properties can exhibit a variety of bifurcation modes. Partly motivating the bifurcation study presented here is one example of such a layered solid, a 100% pearlitic steel which consists of pearlite colonies, each composed of alternating carbide and ferrite plates. Observations of pearlite subjected to overall uniaxial tension reveal that micro-crack initiation appears to result from one of two differing colony-scale bifurcation modes: a periodic, symmetric necking of the carbide plates, and shear band formation in the ferrite[1]. This varying behavior, which can be linked to the metallurgical treatment, is of some interest since the carbide necking mode leads to higher overall ductilities than does shear banding.

Our intention here is to study the conditions under which periodic, symmetric necking modes akin to those observed in pearlite can emerge, and to compare these conditions with those for shear band formation. Such modes appear to be the relevant ones in pearlite, perhaps because modes involving gross shape changes, for example overall bending of the colony, are ruled out by the constraints imposed by adjacent colonies. Bifurcation modes of a layered solid have also been studied by Triantafyllidis and Maker[2], who admit a wide variety of modes, not only those with a periodicity identical to the layering. Our contention, however, is that while the modes admitted in [2] could be observed (and at a lower strain) in an infinite, unconstrained solid, a finite, constrained colony is forced to admit only the modes contemplated here.

A preliminary study of the competition between necking and shear banding was carried out by Steif[3], who investigated the emergence of plane strain undulations at bimaterial interfaces. He considered an infinite solid composed of a single layer of one material, sandwiched between and bonded to half-spaces of a different material, which is subjected to a uniform, in-plane straining parallel to the interface. Inferences concerning the effect of material properties on the competition between modes were drawn from studying the conditions under which undulations confined to the interfaces can appear prior to the equations losing ellipticity, a signal that localized shearing can occur. As seen below, the undulatory modes studied in [3] correspond to the periodic, symmetric necking modes of a layered solid in the limit as one layer becomes very thick compared to the other.

## 2. FIELD EQUATIONS

The infinite, layered solid to be considered is shown schematically in Fig. 1; the alternating layers are labelled A and B. Materials A and B are time-independent and incompressible, and the layers are perfectly bonded. Up to the current instant under consideration, the solid has been subjected to a uniform in-plane straining with the principal stretches parallel with the $x_1$- and $x_2$-axes. The materials are assumed to be incrementally

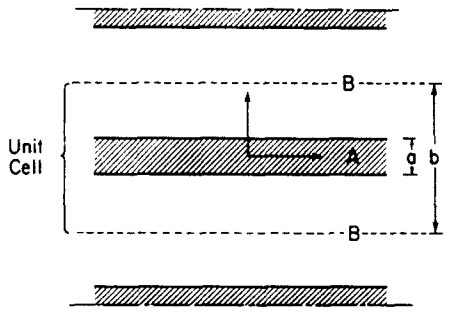


Fig. 1. Schematic of infinite layered composite.

orthotropic, with the incremental deformations from the current state taken to be related to the stress rates according to [4]

$$\overset{\nabla}{\sigma}_{11}-\overset{\nabla}{\sigma}_{22}=2\mu^*(\varepsilon_{11}-\varepsilon_{22}) \qquad \overset{\nabla}{\sigma}_{12}=2\mu\varepsilon_{12}$$

where $\varepsilon_{\alpha\beta}$ are Cartesian components of the Eulerian strain-rate, $\overset{\nabla}{\sigma}_{\alpha\beta}$ are the components of the Jaumann derivative of the true (Cauchy) stress, and subscripts $\alpha$ and $\beta$ take on the values 1 and 2. The material is incrementally isotropic when the incremental moduli $\mu^*$ and $\mu$ are equal. The true stresses in the $x_1$–$x_2$ plane at the current instant are taken to be $\sigma_{11}=\sigma$ and $\sigma_{22}=0$ (plane strain, uniaxial tension). Note that $\sigma$ can be different in A and B.

The method of solution follows that given in [3] very closely, with incremental equilibrium expressed in terms of the nominal stress-rate $\dot{n}_{\alpha\beta}$. By virtue of incompressibility, the velocities $v_\alpha$ (displacement increments) are derivable from a stream function $\psi$

$$v_1=\psi_{,2} \qquad v_2=-\psi_{,1}$$

where

$$(\,)_{,\alpha}\equiv\frac{\partial(\,)}{\partial x_\alpha}.$$

Expressing the nominal stress-rates in terms of the velocities, one finds that the incremental deformations satisfy equilibrium if

$$[\mu+\tfrac{1}{2}\sigma]\psi_{,1111}+[4\mu^*-2\mu]\psi_{,1122}+[\mu-\tfrac{1}{2}\sigma]\psi_{,2222}=0. \tag{1}$$

Conditions which enforce continuity of traction-rates and velocities at the interfaces are

$$\left[\!\left[(\mu-\tfrac{1}{2}\sigma)\left(\frac{\partial^2\psi}{\partial x_2^2}-\frac{\partial^2\psi}{\partial x_1^2}\right)\right]\!\right]=0 \tag{2a}$$

$$\left[\!\left[(4\mu^*-\mu-\tfrac{1}{2}\sigma)\frac{\partial^3\psi}{\partial x_1^2\,\partial x_2}+(\mu-\tfrac{1}{2}\sigma)\frac{\partial^3\psi}{\partial x_2^3}\right]\!\right]=0 \tag{2b}$$

$$\left[\!\left[\frac{\partial\psi}{\partial x_1}\right]\!\right]=\left[\!\left[\frac{\partial\psi}{\partial x_2}\right]\!\right]=0 \tag{2c,d}$$

where $[\![\ ]\!]$ denotes the difference in the values of the enclosed quantity at the interface as one approaches from A and from B.

## 3. EIGENMODES

Searching for the emergence of interface undulations, we inquire as to whether there exist incremental deformations (eigenmodes) which are periodic in $x_1$ of the form

$$\psi = f(x_2)\sin\frac{2\pi x_1}{\lambda}.$$

Furthermore, consistent with our intention to investigate the class of bifurcation modes which are relevant to the tensile straining of a pearlite colony, we restrict our search to eigenmodes involving identical, symmetric deformations in all A layers and in all B layers. Such eigenmodes leave the center-line of each layer straight and untranslated, and they produce deformations which are symmetric about each center-line. Eigenmodes satisfying this periodicity in the $x_2$ direction can be expressed in the form

$$f_A(x_2) = \sin\frac{2\pi}{\lambda}\alpha x_2 \qquad 0 < x_2 < \frac{a}{2}$$

$$f_B(x_2) = \sin\frac{2\pi}{\lambda}\beta\left(\frac{b}{2} - x_2\right) \qquad \frac{a}{2} < x_2 < \frac{b}{2}$$

where $\alpha$ and $\beta$ are, in general, complex constants. (Henceforth, $\alpha$ and $\beta$ will not function as subscripts to indicate Cartesian components.) Since the layer deformations are identical and symmetric, it is only necessary to consider

$$0 < x_2 < \frac{b}{2}.$$

Substituting the assumed forms for $\psi$ into the equilibrium equation (1) for A and B, one finds that $\alpha$ and $\beta$ satisfy

$$\alpha^2 = \frac{R_A - 1 \pm i\sqrt{2R_A - 1 - S_A^2}}{R_A - S_A} \qquad \beta^2 = \frac{R_B - 1 \pm i\sqrt{2R_B - 1 - S_B^2}}{R_B - S_B}$$

where $R = \mu/2\mu^*$ and $S = \sigma/4\mu^*$ in each of A and B. Henceforth, a quantity with a subscript (or superscript) A or B refers to the appropriate material.

In what follows, we will focus on the case in which $R > 1$ in A and B, a condition satisfied by most constitutive models for metals. The two relevant regimes are then: the elliptic regime, $S < \sqrt{2R-1}$, and the hyperbolic regime, $\sqrt{2R-1} < S < R$. (A more extensive discussion of the various regimes can be found in the study by Hill and Hutchinson[4] of bifurcation modes in a rectangular block subjected to plane strain tension.) Thus, for a layered solid composed of two materials, there are three relevant combinations of regimes: both materials elliptic; one material elliptic, one material hyperbolic; both materials hyperbolic. Without loss of generality, we will take A to be hyperbolic when only one of the two materials is hyperbolic.

In the elliptic regime we take

$$f_A(x_2) = \mathrm{Re}\left[c\sin\frac{2\pi}{\lambda}\alpha x_2\right] \tag{3a}$$

$$f_B(x_2) = \mathrm{Re}\left[d\sin\frac{2\pi}{\lambda}\beta\left(\frac{b}{2} - x_2\right)\right] \tag{3b}$$

where $c$ and $d$ are complex-valued amplitudes, and Re[ ] denotes the real part of the enclosed quantity.

The constants $\alpha$ and $\beta$ can be expressed in terms of their real and imaginary parts $\alpha = p_A + ir_A$, $\beta = p_B + ir_B$, where $p$ and $r$ for each layer are given by

$$p^2 - r^2 = \frac{R-1}{R-S} \qquad p^2 + r^2 = \sqrt{\frac{R+S}{R-S}}.$$

In the hyperbolic regime we take

$$f_A(x_2) = c_1 \sin\left[\frac{2\pi}{\lambda} p_A x_2\right] + c_2 \sin\left[\frac{2\pi}{\lambda} r_A x_2\right] \tag{4a}$$

$$f_B(x_2) = d_1 \sin\left[\frac{2\pi}{\lambda} p_B \left(\frac{b}{2} - x_2\right)\right] + d_2 \sin\left[\frac{2\pi}{\lambda} r_B \left(\frac{b}{2} - x_2\right)\right] \tag{4b}$$

where $c_1$, $c_2$, $d_1$ and $d_2$ are real amplitudes, and $p$ and $r$ are now given by

$$p^2 - r^2 = \frac{2\sqrt{S^2 - 2R + 1}}{R-S} \qquad p^2 + r^2 = \frac{2(R-1)}{R-S}.$$

When A is hyperbolic and B is elliptic, eqns (3b) and (4a) are used, with the appropriate definitions for $p$ and $r$.

In each of the three cases, the respective forms for $f_A(x_2)$ and $f_B(x_2)$ are substituted into the continuity conditions (2). Lengthy, though straightforward, manipulations similar to those outlined in [3] are then required to establish the conditions under which there exists a non-trivial solution to the incremental equations. This bifurcation condition depends on the material properties $R_A$, $S_A$, $R_B$, $S_B$, $\xi \equiv \mu_B^*/\mu_A^*$, and the dimensionless wavenumbers $q_A = \pi a/\lambda$ and $q_B = \pi(b-a)/\lambda$. The bifurcation conditions for the three combinations of regimes are found in the Appendix. Previous results[3, 4] are reproduced by taking the appropriate limits of $\xi$, $q_A$ and $q_B$.

## 4. RESULTS AND DISCUSSION

Calculations are first carried out taking materials A and B to be isotropic, incompressible, hyperelastic solids. This particular choice of constitutive model for metals is consistent with accumulating evidence (see Hutchinson[5]) that predictions of bifurcation phenomena depend rather sensitively on the precise constitutive model employed. Generally, the adoption of a flow theory with a smooth yield surface tends to lead to unrealistically high predictions of bifurcation strains. On the other hand, models which incorporate a yield surface vertex and, hence, a more compliant response to non-proportional stress increments result in more realistic estimates of bifurcation strains. The incremental moduli derived from a deformation theory of plasticity (and, in particular, a hyperelastic solid) can represent the moduli for the total loading regime at a yield surface vertex. In particular, we take the relation between true-stress and logarithmic strain to be

$$\sigma = k\varepsilon^N \tag{5}$$

in plane strain tension, where the stiffness $k$ and the hardening rate $N$ generally take on different values in materials A and B. After nondimensionalizing the equations, the independent parameters are $N_A$, $N_B$ and $k_r \equiv k_B/k_A$. For this constitutive law, the quantities $R$, $S$ and $\xi$ are given by

$$R = \frac{\varepsilon}{N}\coth(2\varepsilon) \quad S = \frac{\varepsilon}{N} \qquad \xi = k_r \frac{N_B}{N_A} \varepsilon^{(N_B - N_A)}.$$

The previous study[3], which considered the same material law and corresponds to taking $q_B \to \infty$ in the present calculation, revealed that when either A or B is much stiffer than the other ($k_r \ll 1$ or $k_r \gg 1$), the bifurcation behavior generally is similar to that exhibited by the stiffer solid alone. Undulation bifurcations can occur while both materials are still elliptic, provided the hardening rate of the more compliant solid is not too low. When the hardening rate of the more compliant solid is significantly less than that of the stiffer solid, shear bands in the more compliant solid always precede undulation modes. The general trend was for similar hardening rates and dissimilar stiffnesses to promote undulations over shear banding.

Identical trends were found here when the layer thickness ratio $(b-a)/a$ was taken to be large, but finite. Here, we focus on the influence of varying $(b-a)/a$. Consider the curves shown in Fig. 2, corresponding to a case of dissimilar hardening rates. Clearly, there is no dependence on the thickness ratio when the wavelength is short compared with the layer thicknesses. In fact, the thickness ratio only has an influence when the wavelength exceeds a value that seems to scale with the layer thickness ratio. For example, when $(b-a)/a = 7.0$ (the thickness ratio of ferrite to carbide in pearlite), the previous results are essentially reproduced, provided the wavelength is less than 14 times the thickness of layer A. For longer wavelengths, the assumption that B is semi-infinite leads to an underestimation of the bifurcation strain. This trend continues as $(b-a)/a$ is reduced, with the semi-infinite results significantly underestimating the bifurcation strain over an increasing range of wavelengths.

The same dependence on relative layer thickness appears when the hardening rates are similar: the undulation bifurcation strain generally increases as the relative thickness of the more compliant layer decreases. One can explain this trend as follows. The stiffer layer, say A, dictates the shape of the bifurcation mode; the more compliant layer merely deforms to accommodate the developing neck in such a way that its mid-plane remains stationary. For a given amplitude of the bifurcation mode, the transverse strains $\varepsilon_{22}$ required to accommodate the necking increase as the thickness of the more compliant layer decreases.

As the wavelength becomes very long compared with the layer thicknesses ($q_A \to 0$ and $q_B \to 0$), the strain at which undulation bifurcations occur rises without bound. This was observed in the previous study[3], though it was then thought that this long wavelength behavior was a consequence of assuming layer B was semi-infinite. If one substitutes eqn (3) or (4) into the displacement continuity conditions (2c) and (2d), and lets $q_A$ and $q_B$ both approach zero, one readily sees that the eigenmode must have zero displacement at the interfaces. A more physical appreciation of this point is obtained by considering some point at the interface, say (0, $a/2$), before bifurcation. Without loss of generality, take the incremental strain $\varepsilon_{11}$ of the contemplated eigenmode to be positive. Continuity of dis-

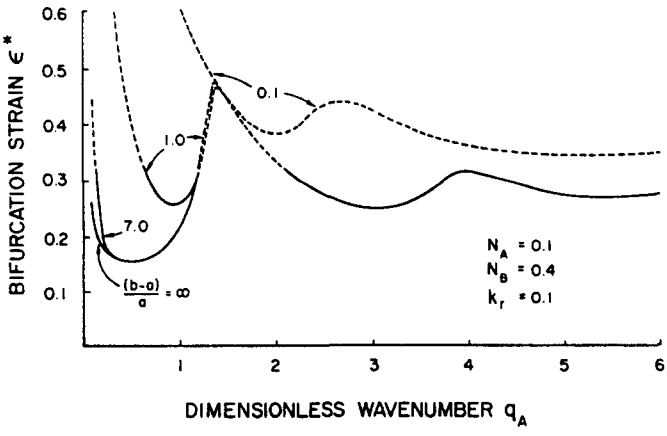


Fig. 2. Dependence of bifurcation strain on relative thickness ratio $(b-a)/a$ for a case of dissimilar hardening rates (—— A and B elliptic, – – – A hyperbolic, B elliptic).

placements and incompressibility imply that $\varepsilon_{22}$ is continuous across the interface and is negative. Now, because the layer center-lines at $x_2 = 0$ and $x_2 = b/2$ do not translate in the periodic, symmetric modes considered here, either layer A or layer B must be expanding along the line $x_1 = 0$; hence, the incremental strain $\varepsilon_{22}$ changes sign in one of the layers. Note also that the incremental stresses and strains of a bifurcation mode vary in a direction normal to the layer over a length scale of the wavelength $\lambda$. In particular, as the wavelength becomes long compared with one or both layers, the incremental strains cannot vary significantly over the thickness and certainly cannot change sign. Thus, the kinematic restrictions of incompressibility and displacement continuity at the interface preclude periodic, symmetric bifurcations with wavelengths greatly in excess of either of the layer thicknesses.

This corrects the previous contention[3] that the long wavelength behavior was a consequence of taking B to be semi-infinite. Unpublished work[6] on compressible materials suggests that removing the incompressibility constraint makes long wavelength bifurcations possible. One interesting consequence of the long wavelength behavior is that one undulatory mode of a definite wavelength would emerge before all others. For a relatively narrow stiffer layer, this wavelength is five to ten times the thickness of the stiffer layer. This is in contrast to necking bifurcations in an isolated block[4] for which the longest wavelength mode consistent with the applied loading is predicted to emerge first.

We close by investigating briefly the effect of changing the constitutive description slightly. Instead of the hyperelastic law, we consider the hypoelastic deformation theory employed by Storen and Rice[7] in their study of sheet necking. Given the same uniaxial stress–strain relation, the hypoelastic and hyperelastic versions coincide when the principal stretch directions remain fixed relative to the material. The hypoelastic version is even more compliant with respect to non-proportional stress increments than is the hyperelastic version. For in-plane deformations, the quantities $R$ and $S$ are now given by

$$R = \frac{1}{2N} \qquad S = \frac{\varepsilon}{N}$$

where again we have specialized to the power law stress–strain relation (5). It is required that $N < 0.5$ and $\varepsilon < 0.5$ for the bifurcation equations given in the Appendix to be valid. Note the two models coincide for infinitesimal strains.

Consistent with other studies that have compared these two constitutive models, the hypoelastic model was here found to lead to slightly lower bifurcation strains. In Fig. 3 we compare the models for two distinct sets of material parameters. The difference between the two models is very slight in the case when $k_r = 0.1$, i.e. when undulation bifurcations occur with both A and B elliptic, and at relatively small strains. The differences between

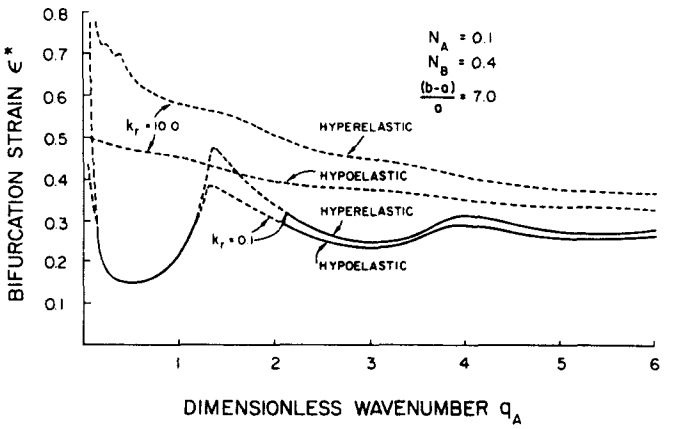


Fig. 3. Comparison of hyperelastic and hypoelastic constitutive laws (——A and B elliptic, – – – A hyperbolic, B elliptic).

the models are more evident at the higher strains at which undulations emerge when the stiffer layer has a high hardening rate. This difference appears not to be very significant insofar as both theories predict shear bands to precede undulation bifurcations.

With the results of the present study and the previous one[3], one may speculate as to the competition between necking and shear band modes in pearlite. One can interpret the carbide layer as the relatively thin, stiff layer and the ferrite as the more compliant thick layer. Shear banding in the ferrite could occur before carbide necking if the hardening rate of the ferrite was sufficiently low. Furthermore, there is a preferred carbide necking mode which has a wavelength which scales with the layer thicknesses, independent of the overall colony size.

*Acknowledgement*—This work has been supported in part by the Association of American Railroads through the Affiliated Laboratory at Carnegie-Mellon University and by the Department of Mechanical Engineering, Carnegie-Mellon University.

## REFERENCES

1. D. J. Alexander and I. M. Bernstein, Microstructural control of flow and fracture in pearlite steels. In *Phase Transformations in Austenite* (Edited by A. R. Marder and J. Goldstein), p. 243. TSM, Warrendale, Pennsylvania (1984).
2. N. Triantafyllidis and B. N. Maker, On the comparison between microscopic and macroscopic instability mechanisms in a class of fiber reinforced composites. *J. appl. Mech.* **52,** 794 (1985).
3. P. S. Steif, Bimaterial interface instabilities in plastic solids. *Int. J. Solids Structures* **22,** 195 (1986).
4. R. Hill and J. W. Hutchinson, Bifurcation phenomena in the plane tension test. *J. Mech. Phys. Solids* **23,** 239 (1975).
5. J. W. Hutchinson, Plastic buckling. In *Advances in Applied Mechanics* (Edited by C.-S. Yih), p. 67. Academic Press, New York (1974).
6. P. S. Steif, unpublished work.
7. S. Storen and J. R. Rice, Localized necking in thin sheets. *J. Mech. Phys. Solids* **23,** 421 (1975).

## APPENDIX

The bifurcation equations are given in this Appendix for the three combinations of deformation regimes in A and B. The notation of the subsequent bifurcation formulae is considerably simplified by defining the following quantities:

$$s_p = \sin(2pq) \qquad s_r = \sinh(2rq) \qquad c_p = \cos(2pq) \qquad c_r = \cosh(2rq)$$

$$Q_p = \sin(pq) \qquad Q_r = \sin(rq) \qquad W_p = p\cos(pq) \qquad W_r = r\cos(rq)$$

$$X = \sqrt{\frac{R+S}{R-S}}.$$

Each of the above quantities takes on a subscript or superscript A or B, depending on the layer.

Case (i): A and B elliptic.

$$(R_A-S_A)\left\{[(1-S_A)X_A-S_A]\frac{s_p^A}{p_A}+[(1-S_A)X_A+S_A]\frac{s_r^A}{r_A}\right\}\left\{\frac{s_p^B}{p_B}-\frac{s_r^B}{r_B}\right\}+(R_B-S_B)\xi^2$$
$$\times\left\{[(1-S_B)X_B-S_B]\frac{s_p^B}{p_B}+[(1-S_B)X_B+S_B]\frac{s_r^B}{r_B}\right\}\left\{\frac{s_p^A}{p_A}-\frac{s_r^A}{r_A}\right\}-\xi\Bigg[(1-S_A)(1-S_B)\left\{\frac{s_p^A}{p_A}-\frac{s_r^A}{r_A}\right\}\left\{\frac{s_p^B}{p_B}-\frac{s_r^B}{r_B}\right\}$$
$$+4(R_A-S_A)(R_B-S_B)[p_As_p^A+r_As_r^A][p_Bs_p^B+r_Bs_r^B]+2(1-S_A)(R_B-S_B)\left\{\frac{s_p^A}{p_A}-\frac{s_r^A}{r_A}\right\}[p_Bs_p^B+r_Bs_r^B]+2(1-S_B)$$
$$\times(R_A-S_A)\left\{\frac{s_p^B}{p_B}-\frac{s_r^B}{r_B}\right\}[p_As_p^A+r_As_r^A]+2(R_A-S_A)(R_B-S_B)\{X_A[c_p^A+c_r^A][c_r^B-c_p^B]+X_B[c_p^B+c_r^B][c_r^A-c_p^A]\}\Bigg]=0.$$

Case (ii): A hyperbolic, B elliptic.

$$(R_A-S_A)^2[(1-p_A^2)^2W_r^AQ_p^A-(1-r_A^2)^2W_p^AQ_r^A][r_Bs_p^B-p_Bs_r^B]$$
$$-2\xi(R_B-S_B)(R_A-S_A)\{[(1-p_A^2)^2W_r^AQ_p^A-(1-r_A^2)^2W_p^AQ_r^A][r_B(1+X_B)s_p^B+p_B(X_B-1)s_r^B]$$
$$-p_Br_B(p_A^2-r_A^2)[W_p^AW_r^A(c_r^B-c_p^B)+X_BQ_r^AQ_p^A(c_r^B+c_p^B)]\}$$
$$+2\xi^2(R_B-S_B)[W_r^AQ_p^A-W_p^AQ_r^A]\{r_B[(1-S_B)X_B-S_B]s_p^B+p_B[(1-S_B)X_B+S_B]s_r^B]\}=0.$$

Case (iii): A and B hyperbolic.

$$
\begin{aligned}
&(R_A - S_A)^2[(1-p_A^2)^2 W_r^A Q_p^A - (1-r_A^2)^2 W_p^A Q_r^A][W_r^B Q_p^B - W_p^B Q_r^B] \\
&\quad - 2(R_A - S_A)(R_B - S_B)\xi\{(1-p_A^2)(1-p_B^2) W_r^A W_r^B Q_p^A Q_p^B + (1-r_A^2)(1-r_B^2) W_p^A W_p^B Q_r^A Q_r^B \\
&\quad - [(1-p_A^2)(1-r_B^2) W_r^A W_p^B Q_p^A Q_r^B + (1-r_A^2)(1-p_B^2) W_r^B W_p^A Q_r^A Q_p^B] \\
&\quad + \tfrac{1}{2}(p_A^2 - r_A^2)(p_B^2 - r_B^2)[W_r^A W_p^A Q_r^B Q_p^B + W_r^B W_p^B Q_r^A Q_p^A]\} \\
&\quad + (R_B - S_B)^2 \xi^2[(1-p_B^2)^2 W_r^B Q_p^B - (1-r_B^2)^2 W_p^B Q_r^B][W_r^A Q_p^A - W_p^A Q_r^A] = 0.
\end{aligned}
$$